

Thalidomide Alleviates Apoptosis, Oxidative Damage and Inflammation Induced by Pemphigus Vulgaris IgG in HaCat Cells and Neonatal Mice Through MyD88

Chunyan Luan^{1,*}, Zhipeng Lu^{2,*}, Juan Chen³, Mengxing Chen¹, Ran Zhao¹, Xiaolan Li¹

¹Department of Dermatology, The Second Affiliated Hospital of Kunming Medical University, Kunming, People's Republic of China; ²Southwest United Graduate School, Yunnan University, Kunming, Yunnan, 650500, People's Republic of China; ³Department of Rheumatology and Immunology, The Second Affiliated Hospital of Kunming Medical University, Kunming, People's Republic of China

*These authors contributed equally to this work

Correspondence: Xiaolan Li, Department of Dermatology, The Second Affiliated Hospital of Kunming Medical University, 374# Dianmian Avenue, Wuhua District, Kunming, Yunnan, People's Republic of China, Tel +86 13629684648, Email prolixl@163.com

Purpose: Thalidomide (Tha) can be used as a selective treatment for mild pemphigus vulgaris (PV). However, the specific mechanism of action remains unclear.

Patients and Methods: PV IgG extracted from patients' serum was cocultured with HaCaT cells to construct a PV cell model, and different concentrations of Tha were used to screen the drug effect. The expression level of MYD88 was assessed in skin lesions of PV patients. Intracellular Ca²⁺ concentration, reactive oxygen species level, DSG3, PG, MYD88, apoptosis-related proteins (Caspase-3, Bcl-2, and Bax), NF-κB pathway-related proteins (IκBα, p-IκBα, p50, and p65), NLRP3, IFN-γ, TNF-α, IL-6, and IL-8 levels were measured. PV IgG was subcutaneously injected into C57BL/6 neonatal mice to construct the animal model. Immunofluorescence was used to detect IgG deposition in the mouse epidermis, whereas immunohistochemistry and TUNEL methods were used to detect the expression of MYD88 and NLRP3 as well as cell apoptosis level in the mouse epidermis.

Results: Tha reversed the decrease in Dsg3 and PG caused by PV IgG. The expression of MyD88 increased in the patients' skin, PV cell model, and PV mouse model. The increase in MyD88 expression level in PV cell models and PV newborn mouse models was inhibited by Tha. Overexpression of MyD88 induced a decrease in the expression levels of Dsg3 and PG in HaCat cells. Overexpression of MyD88 inhibited Tha effects on Dsg3 and PG expressions and blocked Tha effects on Ca²⁺, apoptosis, Bax, Bcl-2, and Caspase-3 expressions, oxidative damage, and inflammatory response in HaCat cells. Tha alleviated acantholysis induced by PV IgG in model mice.

Conclusion: Through MYD88, Tha attenuated apoptosis of HaCat cells, modulated NF-κB to hamper the oxidative damage and inflammatory response in the PV cell models, and alleviated acantholysis, IgG deposition, and epidermal cell apoptosis induced by PV IgG in model mice.

Keywords: pemphigus vulgaris, thalidomide, oxidative damage, apoptosis, inflammation, MyD88

Introduction

Pemphigus refers to a group of severe autoimmune skin disorders that can threaten patients' health and life, mainly manifesting as loose blisters and bullae on the skin that easily rupture. The patient's serum can be examined for the presence of antibodies directed against intercellular desmosome structures, including desmoglein 1 (Dsg1) and desmoglein 3 (Dsg3). The pathological feature of pemphigus is Nikolsky's sign, which refers to the destruction of acanthocytes adhesions in the skin and mucous membranes due to the binding of autoantibodies to acanthocytes and subsequent attack on desmosomal proteins.^{1,2} In clinical practice, pemphigus is mainly divided into two types based on the location of blister formation in the epidermis, clinical features, and target antigens: pemphigus vulgaris (PV) and pemphigus foliaceus (PF).³ PV is the most prevalent and severe type of pemphigus, representing 70% of all disease cases.

The current treatment strategy for PV is the systemic combination of corticosteroids and immunosuppressive agents. However, long-term high-dose or irregular use of glucocorticoids can predispose patients' to infections and aggravate existing infections, as well as cause adverse reactions such as osteoporosis, aseptic necrosis of the femoral head, peptic ulcers, hyperlipidemia, water and sodium retention, and even death in severe cases.⁴ The utilization of rituximab in recent years has resulted in enhanced treatment effectiveness among individuals with PV.⁵ However, like other glucocorticoids and immunosuppressants, rituximab can increase the risk of developing bacterial and viral infections, requires a long treatment cycle, and is expensive, thus, limiting its use options for most patients.

Thalidomide (Tha), which is an immunomodulatory and anti-inflammatory glutamic acid derivative, has demonstrated efficacy in treating various chronic inflammatory skin diseases, including pyoderma gangrenosum, actinic prurigo, lupus erythematosus, aphthous stomatitis, and prurigo nodularis.⁶ Previous studies have reported multiple cases of paraneoplastic pemphigus treated with Tha alone or with Tha combined with glucocorticoids, and all patients achieved significant remission.⁷ In a clinical study by LiLi in which 6 PV patients were treated with Tha alone, Pemphigus Disease Area Index (PDAI) of them ranged from 1 to 24. The damage to the skin and mucous membrane was significantly reduced, suggesting that Tha can be used as an optional therapy for mild PV as well as considered an alternative therapy for mild pemphigus.⁸ Nevertheless, the specific mechanism of action is yet to be studied.

Myeloid differentiation primary response gene 88 (MyD88) is an intracellular adaptor protein. It serves as a typical adaptor between Toll-like receptor (TLR) and interleukin-1 (IL-1) receptor families downstream of the inflammatory signaling pathway. The overexpression of MyD88 leads to increased Ca^{2+} concentrations, increased reactive oxygen species (ROS), and activation of the NF- κ B signaling pathway, which produces proinflammatory factors and promotes oxidative damage and inflammation.⁹

Studies have shown that Tha can downregulate the expression of MyD88.¹⁰ In the current research, the expression of Myd88 in the skin lesions of patients was explored. Through cell and mouse experiments, it was found that Tha downregulated the expression of Myd88 and inhibited apoptosis and oxidative damage of epidermal cells in a PV cell model as well as inhibited inflammation and alleviated acantholysis and ulceration of the skin in a PV mouse model. These findings provide a theoretical foundation for Tha as a potential therapeutic target to treat mild pemphigus.

Materials and Methods

Drugs and Reagents

HaCat cells were supplied by the Chinese Academy of Sciences (China). Tha was obtained from Sigma-Aldrich Corp (USA). Antibodies against Dsg3, plakoglobin (PG), p-I κ B (S32), NLRP3, and MyD88 were supplied by Abcam (Abcam, Cambridge, USA). Antibodies against NF- κ B (p65), I κ B, Caspase-3, Bax, Bcl-2, and β -actin were supplied by Proteintech Group (Proteintech Group, Inc, USA). SK&F 96365 and BAY11-7082 were purchased from Selleckchem (Selleck Chemicals).

Patients

Serum and skin samples were obtained from six PV patients (PV1, PV2, PV3, PV4, PV5, and PV6) (PV IgG) and six healthy humans (NH IgG). Eligible PV patients included those with newly diagnosed or relapsing PV, It was diagnosed based on positive direct immunofluorescence showing IgG deposits on the surface of acanthocytes and positive Dsg-1/3 enzyme-linked immunosorbent assay (ELISA). In this experiment, we mainly wanted to obtain high concentrations of IgG from patient serum, so the Pemphigus Disease Area Index (PDAI) ranged from 24 to 45. All patients provided informed consent. The study was performed according to the Declaration of Helsinki. Pathogenicity experiments were positively reviewed by the ethics committees of the Second Affiliated Hospital of Kunming Medical University (no. Shen-PJ-2021-168).

Affinity Purification of PV IgG and NH IgG

rProtein G Beads were loaded into an appropriate chromatographic column and equilibrated five times according to the column volume of the equilibration solution, ensuring that the packing material was under the same buffer system as the target protein for protection, to purify anti-IgG through immunoaffinity. The sample was added to the equilibrated rProtein G Beads to ensure sufficient contact between the target protein and rProtein G Beads for improving the recovery of the target protein, and the effluent (filtrate) was collected. The column was washed with 30 mL of washing solution to remove any nonspecifically adsorbed heteroproteins, and the resulting washing solution was collected.

The protein was eluted using 15–30 mL of eluate. The eluate was collected in sections, and the concentration of the eluate was detected by an enzyme marker. Centrifugal concentration was performed for 30 min using a 100-k ultrafiltration tube. Protein quantification was performed using the Enhanced BCA Protein Assay Kit (Beyotime, P0010) according to the manufacturer's instructions. Ultimately, Dsg3/1-depleted PV IgG and anti-Dsg3 PV IgG were assessed for anti-Dsg3 and anti-Dsg1 autoantibody reactivity by ELISA (Euroimmun). Dsg3 antibody titer was 653 U/mL, and Dsg1 antibody titer was 343 U/mL.

Cell Structure and Treatment

HaCaT cells, a human epidermal keratinocyte cell line, were grown in 10% fetal bovine serum (Biological Industries, South American source)-supplemented RPMI 1640 (Corning, USA). Antibiotics (100 mg/mL streptomycin and 100 IU/mL penicillin) were added to the media, and the mixture was kept in a humidified environment comprising 95% air and 5% CO₂ at 37 °C.

At a density of 4×10^4 cells per well, a 6-well plate was utilized to seed HaCaT cells. The cells were treated with phosphate-buffered saline (PBS), 1000 µg/mL NH IgG, PV IgG, Tha, SK&F 96365 (10 µmol/L), and BAY11-7082 (5 µmol/L) under various conditions. pCDH-MyD88 vectors (pCDH-MyD88-1 and pCDH-MyD88-2) and negative control vector (acquired from GeneParma Co., Ltd [Shanghai, China]) were transfected into cells.

Analysis of Apoptosis Through Flow Cytometry

Flow cytometry was performed using a FITC-labeled recombinant Annexin V apoptosis detection kit (Beyotime, China). Either treated or untreated cells were harvested continuously, washed in PBS, and reconstituted in a coupling buffer (10 mM HEPES/NaOH, pH 7.4, 2.5 mM CaCl₂, 140 mM NaCl). Annexin V-FITC was introduced (at 250 ng/mL final concentration) before incubation in the darkness at 4 °C for 15 min, followed by washing with PBS and resuspension in 190 µL coupling buffer. Then, 10 µL of propidium iodide (PI) was added for 5 min. Stained cells were examined by a FACStar plus flow cytometer (Becton Dickinson, USA). The ratio of fluorescence intensities that were excited at 488 nm was monitored at an emission wavelength of 515 nm and 560 nm for FITC and PI, respectively. The collected data were analyzed with a BD BioSciences FACSCalibur flow cytometer using CellQuest software.

Measurement of Intracellular Calcium

A fluorescence microscope and Rhod-2 dye were utilized as a fluorescent probe allowed for the detection of intracellular calcium ion accumulation. HaCaT cells were incubated with media containing NH IgG (1000 µg/mL), PV IgG (1000 µg/mL), Tha (5 µg/mL), pcdh-MyD88, and SK&F 96365 (10 µmol/L), respectively. The cells in the control group were incubated in media with the same PBS volume. Following 48 h of treatment, the media was removed, with subsequent staining of the cells for 60 min with 1 µM of Rhod-2 dye. The cells were washed with HBSS thrice and then incubated for 30 min at 37 °C to ensure complete transformation of Rhod-2 dye to Rhod-2 in the cells. Finally, fluorescence was captured using a fluorescence microscope.

Measurement of Intracellular ROS

At a density of 1×10^5 cells/well, the 6-well plate was utilized for the seeding HaCaT cells, followed by transfection with pcdh-MyD88 after 24 h. After reaching confluence, the cells were passaged for 24 h after plating and then treated with PV IgG (1000 µg/mL), Tha (5 µg/mL), and BAY11-7082 (5 µmol/L) for 24 h. The cells were rinsed with serum-free

RPMI 1640 (twice) and stained with 10 mM H2DCFDA for 15 min. The cells were then washed twice with serum-free DMEM and observed under a fluorescence microscope (Nikon, Japan).

Determination of Superoxide Dismutase (SOD), Malondialdehyde (MDA), and Catalase (CAT) Levels

Commercially available MDA, SOD, and CAT kits (Beyotime, China) were used to determine MDA, SOD, and CAT levels in cultured cells. The manufacturer's guidelines were followed for each kit. The data obtained were analyzed utilizing a SpectraMax M5 spectrophotometer (Molecular Devices, USA).

Western Blot Analysis

Utilizing the BCA protein assay reagent (Beyotime, China), the protein concentration was determined after preparing protein lysates utilizing RIPA or Triton X-100. An equal quantity of proteins was separated by SDS-PAGE of 10% for NLRP3, Dsg3, and PG (all 1:1000) and 12% for MyD88, Bcl-2, Bax, Caspase-3, p65, p-I κ B (all 1:1000), I κ B (1:2000), and β -actin (1:10,000). The proteins were then transferred onto a PVDF membrane (Millipore Corporation, USA), followed by overnight soaking at 4 °C in a 5% skimmed milk, PBS, 0.1% Tween-20 (pH 7.2). The membrane was subsequently incubated with a primary antibody, followed by peroxidase-conjugated anti-rabbit or anti-mouse IgG (1:10,000) (Proteintech Group, Inc, USA). ECL Western blot detection kit (Tanon, China) was utilized to visualize the epitope, and the other steps were performed according to the manufacturer's instructions for each antibody.

Quantitative Real-Time Polymerase Chain Reaction (q-PCR)

HaCaT cells were cultured as per the aforementioned procedures. RNAiso Plus reagent (TaKaRa, Japan, cat. no. 108–95-2) was utilized to extract total RNA from the cells according to the manufacturer's guidelines. RevertAid First-strand cDNA Synthesis kit (ThermoFisher Scientific, UAB, K1622) was used to synthesize cDNA. For quantifying NLRP3 expression, q-PCR was conducted on a CFX96 Touch thermocycler (Applied Biosystems) utilizing SYBR[®] Premix Ex Taq[™] II (Applied Biosystems/ThermoFisher Scientific, UAB, A25742). The following primer sequences were used for NLRP3 and β -actin (Sangon Biotech, Shanghai, China):

NLRP3 (forward primer): 5'-CCAGAGCCTCACTGAACTGG-3',

NLRP3 (reverse primer): 5'-AGCATTGATGGGTCAGTCCG-3';

β -actin (forward primer): 5'-CTGTGTGGATTGGTGGCTCT-3',

β -actin (reverse primer): 5'-GCTCAGTAACAGTCCGCCTA-3'.

PCR amplification involved heating the samples at 95 °C for 30 sec, followed by 45 cycles of 95 °C for 5 sec and 55 °C for 30 sec. β -actin was utilized as an endogenous control to normalize differences. A PCR post-data analysis software program was utilized to process fluorescence data. The $2^{-\Delta\Delta CT}$ method was utilized to analyze differences in gene expression.

Animals

Wild-type C57BL/6 pregnant mice were acquired from Kunming Medical University, China. The mice were placed in plastic cages with free access to proper food and water in a 12-h light/dark cycle. This study aimed to determine whether PV IgG could induce PV in mice. Therefore, neonatal mice were classified into three groups (n=6 per group) as follows: control, NH IgG, and PV IgG groups. Mice in the control group received only PBS. Mice in the NH IgG group received a subcutaneous injection of NH IgG (1.5 mg/g). Mice in the PV IgG group received a subcutaneous injection of PV IgG (1.5 mg/g). For Tha treatment, four groups of neonatal mice were established (n=6 per group): PV IgG, Tha (10 mg/kg), Tha (20 mg/kg), and Tha (50 mg/kg) groups. Neonatal mice received intraperitoneal injections of Tha for 8 days (10, 20, and 50 mg/kg once a day). Then, mice in all groups received a subcutaneous injection of PV IgG (1.5 mg/g). The animal ethics council of Kunming Medical University approved all protocols and procedures used in the study. These procedures were conducted according to the National Institutes of Health Guide for the Care and Use of Laboratory Animals and were approved by the local Committee on Animal Use and Protection of Yunnan province (License No. LA2008305).

Sample Size Calculation

The “resource equation method” is indeed an alternative approach used to determine sample sizes in experiments, considering the law of diminishing returns. This method is particularly useful for biological experiments and animal studies with multiple treatment groups and a small sample size that require analysis through analysis of variance (ANOVA). The “resource equation method” establishes an acceptable range for error degrees of freedom in ANOVA, which is generally between 10 and 20. The equation mentioned to determine the total number of observations (N) is as follows: $N = (X-1+B+T)$, where T represents the number of treatments, B represents the number of blocks, and X should be within the range of 10 to 20. In the case of in vivo research, B is equal to 4 and T is equal to 1. Therefore, the calculation would be: $N = (14 \text{ to } 24)$. By dividing 24 by 4, we get 6. Therefore, the determined sample size for each experimental group in this case would be 6.

Elisa

ELISA kits (Biolegend) were used to measure the levels of cytokines (TNF- α , IL-1 β , and IL-6) in the culture media of various treatment groups. Each experiment is representative of at least five independent experiments.

Hematoxylin-Eosin (H&E) Staining

After quickly removing the skin from mice, the samples were post-fixed, paraffinized, and cut into 5 μm -thick sections. Two rounds of xylene treatment (each for 10 min) were utilized for dewaxing the samples with subsequent rehydration in two rounds of absolute ethanol (each for 5 min), followed by orderly rinsing with tap water. The sections underwent H&E staining to observe the histomorphology. An investigator blinded to the study groups performed the histology assessment.

Immunohistochemistry

Skin sections were incubated overnight with MyD88 and NLRP3 primary antibodies (1:100 dilution) at 4 °C. Then, the sections were subjected to incubation with a biotinylated anti-rabbit IgG secondary antibody (1:500 dilution), followed by signal development via DAB staining. Finally, the sections were examined and imaged using a light microscope.

Immunofluorescence

HaCaT cell slides were incubated with Dsg3 and PG primary antibodies (1:300 dilution) at 4 °C overnight. Afterward, slices were incubated with Cy3 conjugated anti-rabbit IgG at a dilution of 1:500 for 1 h at room temperature. Finally, DAPI dye was utilized for staining the slices.

Direct immunofluorescence (DIF)

Neonatal mice skins used as the substrate for DIF were biopsied 3 h after injection. The skin samples were embedded in OCT and sectioned at a thickness of 4–5 μm after being frozen. After fixation with acetone at 4 °C for 10 min, the sections were immersed in 0.01 mol/L PBS (pH 7.4) at 4 °C for 1 min and kept at a specific humidity level. To block each section, 100 μL of 10% goat serum was applied at room temperature for 30 min, followed by washing with 0.01 mol/L PBS (pH 7.4) three times. Each section was treated with rabbit anti-human IgG (H + L)-FITC antibodies at a dilution of 1:200, followed by incubation at 37 °C for 30 min in the darkness and washing four times for 1 min each with PBS. Then, a glass slide was covered with a drop of buffered glycerin. Finally, the images were captured utilizing a fluorescence microscope.

TUNEL Assay

The skin samples from the experimental mice were embedded in OCT. Then, 4% paraformaldehyde in PBS solution was utilized for the fixation of the cryopreserved tissue sections (20 min). The sections underwent TUNEL assay in accordance with the manufacturer’s guidelines utilizing the in situ cell death detection kit (Roche). After

permeabilization and washing, the sections were incubated for 1 h with a reaction mixture containing TdT and fluorescence-conjugated dUTP at 37 °C. A fluorescence microscope was used to examine the labeled DNA.

Statistical Analysis

Statistical analysis was performed using Prism 8.0 (GraphPad). Normal probability plots (Q-Q plot, quantile-quantile plot) and normality test (Shapiro–Wilk test) were used to assess data distribution before conducting any statistical analysis. The homogeneity of the data was assessed with Bartlett's test. Data were expressed as mean \pm standard error of the mean (SEM) from at least five separate experiments. Statistical differences between values were evaluated by One-way ANOVA, followed by a post-hoc Bonferroni multiple comparison test. When the assumption of equal variances is violated, Welch ANOVA was utilized. Differences between different groups were considered significant if the P-value was <0.05 .

Results

Tha Reverses the Decrease in Dsg3 and Plakoglobin (PG) Caused by PV-IgG Extracted from the Serum of the Patient

Decreased expression of Dsg3 and PG is one of the characteristics of pemphigus.¹¹ A cell model of pemphigus was constructed using HaCaT cells, and PV-IgG extracted from the serum of the patient was purified. Different concentrations of PV-IgG were tested. When the concentration of PV-IgG was 1000 $\mu\text{g/mL}$, the protein expression levels of Dsg3 and PG were considerably lower than those in the NH-IgG group (control) (Figures 1A–C). PV-IgG at a concentration of 1000 $\mu\text{g/mL}$ was utilized in subsequent experiments. To further confirm the initial findings, immunofluorescence was utilized to label Dsg3 and PG, and it was found that after HaCaT cells were cocultured with PV-IgG, the fluorescence staining pattern of Dsg3 and PG changed significantly (Figure 1D), the fluorescence intensity decreased, the continuity of fluorescence between cells was disrupted, and Dsg3 and PG were internalized. Subsequently, to observe the effect of Tha on desmosome proteins, HaCaT cells were cocultured with 1000 $\mu\text{g/mL}$ PV-IgG for 24 hours. Following this, 5 $\mu\text{g/mL}$, 10 $\mu\text{g/mL}$, or 50 $\mu\text{g/mL}$ of Tha were added to the cells, and the culture was continued for another 24 hours. Following treatment with 5 $\mu\text{g/mL}$ and 10 $\mu\text{g/mL}$ Tha, the expression of Dsg3 and PG exhibited recovery to a certain extent (Figures 1E–G). The effect in the 5 $\mu\text{g/mL}$ Tha group was strongest, with no recovery in the 50 $\mu\text{g/mL}$ Tha group. Thus, 5 $\mu\text{g/mL}$ Tha was used in subsequent experiments.

Overexpression of MyD88 is Associated with Pemphigus, and Tha Inhibits the Increase in MyD88 Caused by PV-IgG

MyD88 is associated with autoimmune diseases and various skin diseases,¹² and it was hypothesized that MyD88 is also abnormally expressed in pemphigus. After observing MyD88 protein in the cell model, it was found that the MyD88 protein level was elevated in the PV-IgG group than in the NH-IgG group and that the MyD88 level in the PV-IgG group decreased after Tha treatment (Figure 2A and B). Immunohistochemical staining of MyD88 was performed on skin samples obtained from patients, and the results were consistent with those obtained from cellular experiments. MyD88 staining was deeper in skin samples from pemphigus patients than in normal subjects (Figure 2C). To assess the influence of the elevated expression level of MyD88 on desmosome proteins, the two MyD88 overexpression vectors (pCDH-MyD88-1 and pCDH-MyD88-2) were utilized. It was found that the MyD88 expression level in the pCDH-MyD88-1 and pCDH-MyD88-2 groups was considerably elevated and that the expression levels of Dsg3 and PG considerably decreased after MyD88 overexpression (Figure 3A–D). pCDH-MyD88-2 exhibited greater efficacy compared to pCDH-MyD88-1. Hence, it was chosen for further experiments.

This study further explored whether the effect of Tha was achieved through MyD88. The expression levels of Dsg3 and PG were considerably lowered in the PV+pCDH-MyD88+Tha group compared to those in the PV+Tha group (Figures 3E–G). Furthermore, treatment with Tha did not lead to the recovery of the expression levels of Dsg3 and PG, indicating that MyD88 is critically involved in the pathogenesis of pemphigus and that Tha may exert a therapeutic effect by affecting MyD88. This study employed immunofluorescence to detect Dsg3 and PG in HaCaT cells and found that

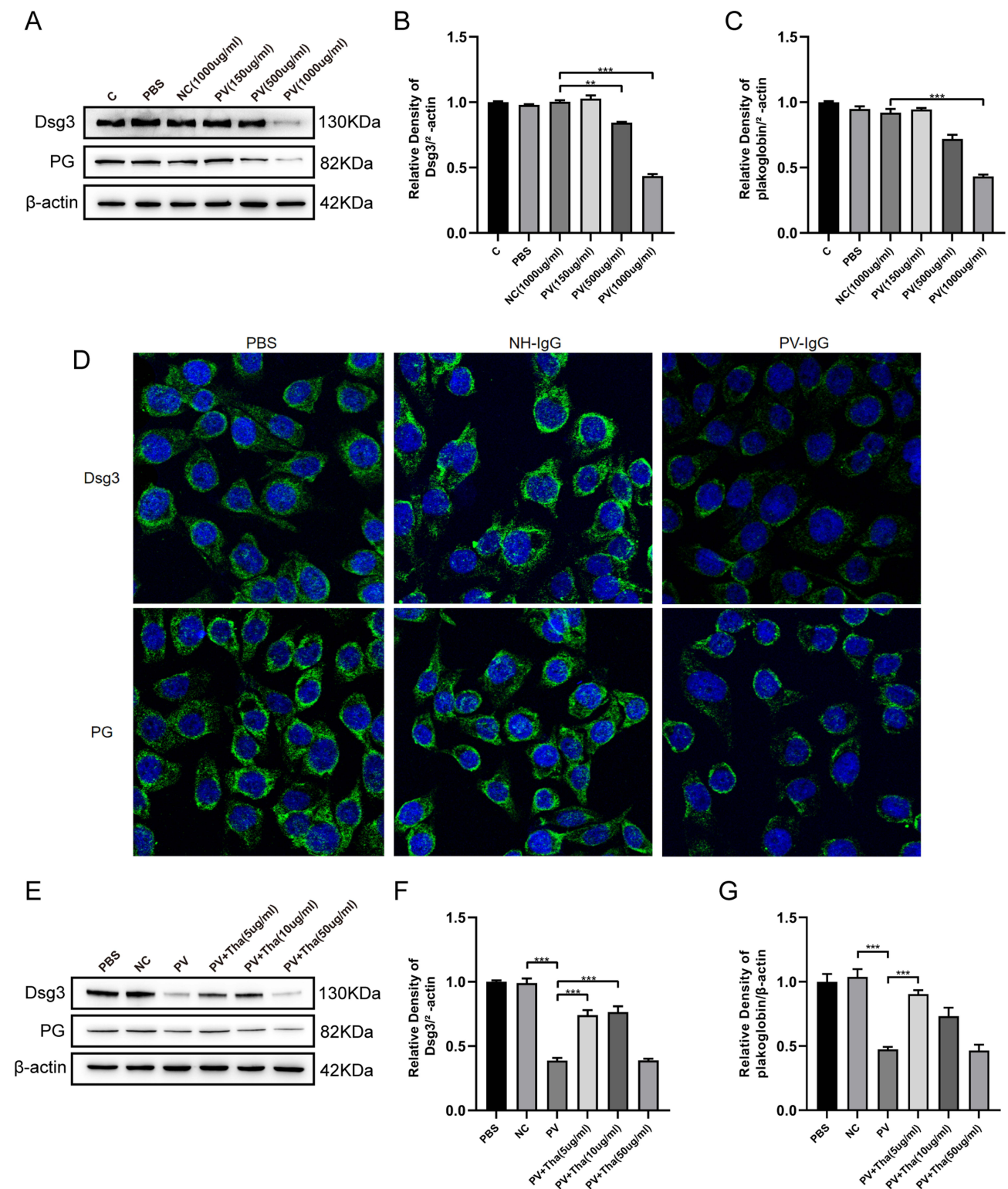


Figure 1 Thd restored the Dsg3 and PG expressions decreased by PV-IgG in HaCat cells. **(A)** HaCat cells were pretreated with PBS, normal human IgG (NC or NH-IgG) 1000 ug/mL, pemphigus vulgaris IgG (PV) 150 ug/mL, 500 ug/mL and 1000 ug/mL differently. Representative Western blots and quantification of indicated proteins in HaCat cells lysate. **(B)** Dsg3 was expressed lower in PV (500 ug/mL and 1000 ug/mL) than NC (1000 ug/mL). **(C)** PG (plakoglobin) was expressed lower in PV (1000 ug/mL) than NC (1000 ug/mL). **(D)** Immunofluorescence (IF) on HaCat cells. PV-IgG from pemphigus vulgaris (PV) patients decreased Dsg3 and PG, compared with NH-IgG. Nuclei were counterstained with DAPI. **(E)** HaCat cells were pretreated with PBS, normal human IgG (NC or NH-IgG) 1000 ug/mL and pemphigus vulgaris IgG (PV) 1000 ug/mL then added Thd 5 ug/mL, 10 ug/mL and 50 ug/mL differently. Representative Western blots and quantification of indicated proteins in HaCat cells lysate. **(F)** PV-IgG-decreased expression of Dsg3 was reversed by Thd (5 ug/mL and 10 ug/mL) in HaCat cells. **(G)** PV-IgG-decreased expression of PG was reversed by Thd (5 ug/mL) in HaCat cells. Relative expression was normalized to control group. Asterisks indicate statistical significance (* $p < 0.05$, ** $p < 0.01$, *** $p < 0.001$). Each experiment is representative of five independent experiments. The data are presented as the mean \pm SEM of five separate experiments.

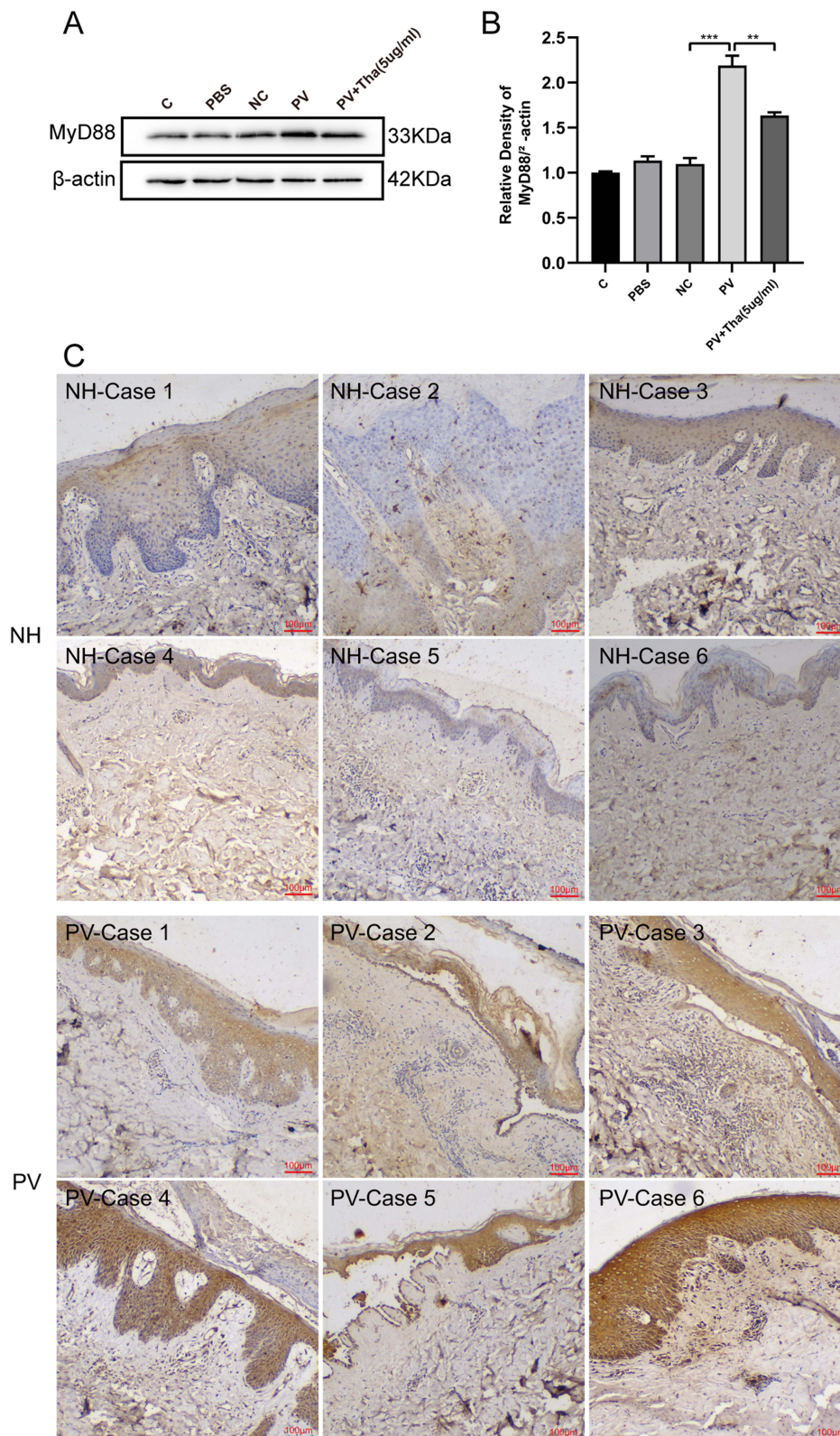


Figure 2 Effects of MyD88 in both PV cell model and patients. **(A)** HaCat cells were pretreated with PBS, normal human IgG (NC) 1000 ug/mL and pemphigus vulgaris IgG (PV) 1000 ug/mL + Thd 5 ug/mL differently. Representative Western blots and quantification of indicated proteins in HaCat cells lysate. **(B)** MyD88 was expressed higher in PV (1000 ug/mL) than NC (1000 ug/mL), and was reversed by Thd. **(C)** Six PV cases and six healthy individual controls were analyzed by immunohistochemistry for MyD88. Positivity of MyD88 staining was detected in PV patients, whereas the healthy control samples showed little or no staining in the skin. Relative expression was normalized to control group. Asterisks indicate statistical significance (** $p < 0.01$, *** $p < 0.001$). Each experiment is representative of five independent experiments. The data are presented as the mean \pm SEM of five separate experiments.

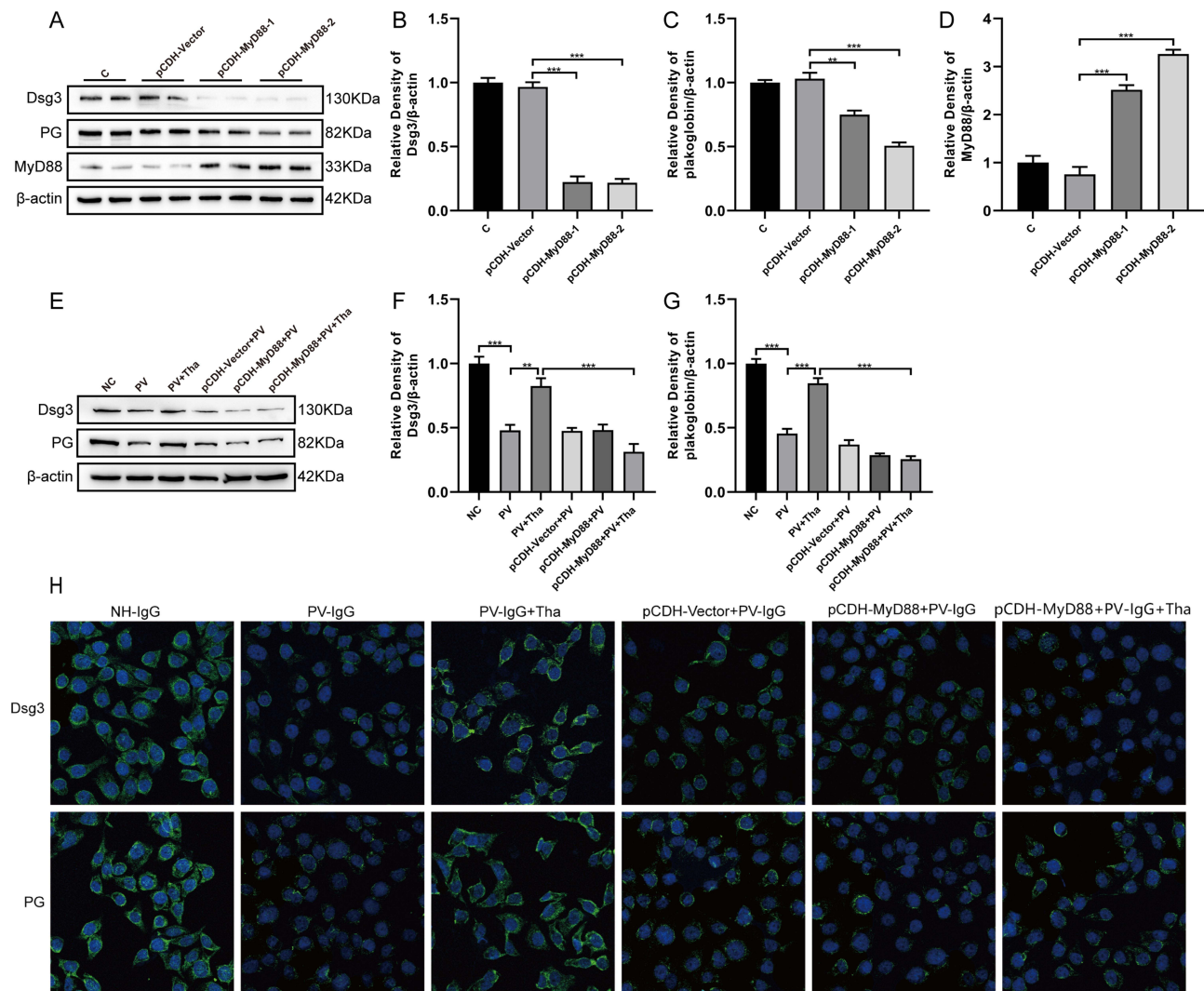


Figure 3 Overexpression of MyD88 inhibited Thd effects on Dsg3 and PG expressions by PV-IgG in HaCat cells. **(A)** HaCat cells were pretreated with p-CDH-Vector, p-CDH-MyD88-1 and p-CDH-MyD88-2 differently. Representative Western blots and quantification of indicated proteins in HaCat cells lysate. **(B)** Overexpression of MyD88 by p-CDH-MyD88-1 and p-CDH-MyD88-2 decreased Dsg3 expression in HaCat cells. **(C)** Overexpression of MyD88 by p-CDH-MyD88-1 and p-CDH-MyD88-2 decreased PG expression in HaCat cells. **(D)** Overexpression of MyD88 by p-CDH-MyD88-1 and p-CDH-MyD88-2 increased MyD88 expression in HaCat cells. **(E)** HaCat cells were pretreated with NH-IgG (NC), PV-IgG (PV), PV-IgG + Thd (PV + Thd), p-CDH-Vector + PV-IgG (p-CDH-Vector + PV), p-CDH-MyD88-2 + PV-IgG (p-CDH-MyD88 + PV) and p-CDH-MyD88-2 + PV-IgG + Thd (p-CDH-MyD88 + PV + Thd) differently. Representative Western blots and quantification of indicated proteins in HaCat cells lysate. **(F)** PV-IgG-decreased expression of Dsg3 was reversed by Thd, overexpression of MyD88 decreased Dsg3 expression, overexpression of MyD88 blocked the effects of Thd on Dsg3 in HaCat cells. **(G)** PV-IgG-decreased expression of PG was reversed by Thd, overexpression of MyD88 decreased PG expression, overexpression of MyD88 blocked the effects of Thd on PG in HaCat cells. **(H)** Immunofluorescence (IF) on HaCat cells. PV-IgG decreased Dsg3 and PG, compared with NH-IgG, Thd restored the PV-IgG-induced decreased of Dsg3 and PG expression, overexpression of MyD88 blocked the effects of Thd on Dsg3 and PG in HaCat cells. Nuclei were counterstained with DAPI. Relative expression was normalized to control group. Asterisks indicate statistical significance (* $p < 0.05$, ** $p < 0.01$, *** $p < 0.001$). Each experiment is representative of five independent experiments. The data are presented as the mean \pm SEM of five separate experiments.

after overexpressing MyD88, the fluorescence staining patterns of Dsg3 and PG changed significantly in HaCaT cells cocultured with PV-IgG (Figure 3H): the fluorescence intensity decreased, and the continuity of fluorescence between cells was disrupted. MyD88 overexpression caused the internalization of Dsg3 and PG and inhibited the role of Tha.

Tha Inhibits Ca^{2+} Influx via MyD88 and Attenuates Apoptosis in Epidermal Cells in a PV Cell Model

Earlier investigations have demonstrated that MyD88 can regulate the intracellular Ca^{2+} concentration by affecting the oxidation of calmodulin-dependent protein kinase II,¹³ thereby affecting cell apoptosis. Fluorescent probes were utilized to detect the amount of intracellular Ca^{2+} , and it was found that the Ca^{2+} content in the PV group was remarkably

elevated than that in the NC group (Figure 4A). After using Tha, the increase in Ca^{2+} was attenuated. Ca^{2+} significantly recovered after MyD88 overexpression, and the increase in Ca^{2+} was attenuated after treatment with the calcium channel blocker SK&F 96365 (10 μ mol/L). The apoptosis rate of cells in each group was assessed by flow cytometry (Figure 4B and C). The PV group exhibited a significantly higher cell apoptosis rate than the NC group.

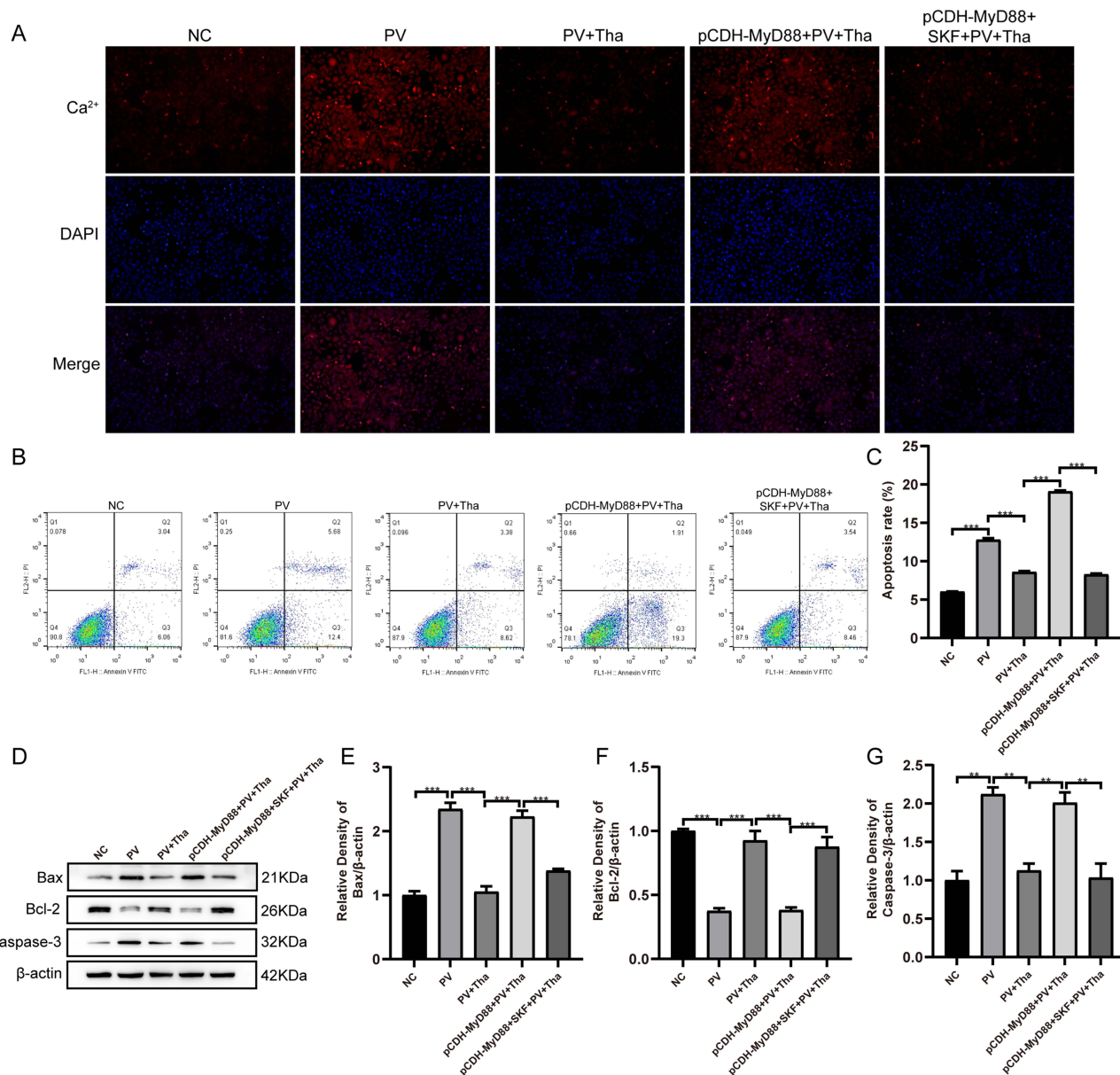


Figure 4 Overexpression of MyD88 blocked Thalidomide effects on Ca^{2+} , apoptosis, Bax, Bcl-2 and Caspase-3 expressions by PV-IgG in HaCat cells. **(A)** HaCat cells were pretreated with NH-IgG (NC), PV-IgG (PV), PV-IgG + Thd (PV+Thd), p-CDH-MyD88-2 + PV-IgG + Thd (p-CDH-MyD88 + PV + Thd) and p-CDH-MyD88-2 + SK&F 96365 (10 μ mol/L) + PV-IgG + Thd (p-CDH-MyD88 + SKF + PV + Thd) differently. Representative fluorescent images of intracellular calcium level in HaCat cells showed red using Rhod-2 dye. The nucleus showed blue using DAPI. PV-IgG-increased the red fluorescent images, was reversed by Thd, overexpression of MyD88 blocked the effects of Thd on red fluorescent, using calcium antagonist SK&F 96365 (10 μ mol/L) inhibited the increased Ca^{2+} by overexpression MyD88 in HaCat cells. **(B)** Detection of apoptotic HaCat cells in different treatment. **(C)** PV-IgG-increased the apoptosis rate, was reversed by Thd, overexpression of MyD88 blocked the effects of Thd on apoptosis rate, using calcium antagonist SK&F 96365 (10 μ mol/L) inhibited the increased apoptosis rate by overexpression MyD88 in HaCat cells. **(D)** Representative Western blots and quantification of indicated proteins in HaCat cells lysate. **(E)** PV-IgG-increased Bax expression, was reversed by Thd, overexpression of MyD88 blocked the effects of Thd on Bax, using calcium antagonist SK&F 96365 (10 μ mol/L) inhibited the increased Bax by overexpression MyD88 in HaCat cells. **(F)** PV-IgG-decreased Bcl-2 expression, was reversed by Thd, overexpression of MyD88 blocked the effects of Thd on Bcl-2, using calcium antagonist SK&F 96365 (10 μ mol/L) inhibited the decreased Bcl-2 by overexpression MyD88 in HaCat cells. **(G)** PV-IgG-increased Caspase-3 expression, was reversed by Thd, overexpression of MyD88 blocked the effects of Thd on Caspase-3, using calcium antagonist SK&F 96365 (10 μ mol/L) inhibited the increased Caspase-3 by overexpression MyD88 in HaCat cells. Relative expression was normalized to control group. Asterisks indicate statistical significance (** $p < 0.01$, *** $p < 0.001$). Each experiment is representative of five independent experiments. The data are presented as the mean \pm SEM of five separate experiments.

After treatment with Tha, the apoptosis rate decreased. After MyD88 overexpression, the apoptosis rate considerably enhanced than that in the Tha+PV group and then decreased after treatment with the calcium channel blocker SK&F 96365 (10 $\mu\text{mol/L}$), consistent with the results for Ca^{2+} . The study detected apoptosis-related proteins and revealed that the protein expression level of Bcl-2 was lower in the PV model group compared to that in the NC group. Additionally, the protein expression level of Caspase-3 and Bax was elevated in the PV model group compared to that in the NC group (Figure 4D–G). After Tha treatment, the protein expression of Bcl-2 increased, and that of Caspase-3 and Bax decreased. Compared with that in the Tha+PV group, the protein expression level of Bcl-2 was lower and the protein expression of Caspase-3 and Bax was higher following treating MyD88-overexpressing PV model HaCaT cells with Tha. The expression of Bcl-2 protein recovered after treatment with SK&F 96365, and Caspase-3 and Bax protein expression decreased.

Tha Regulates NF- κB via MyD88 to Attenuate Oxidative Damage and Inflammatory Responses in Epidermal Cells in a PV Cell Model

The course of PV is closely associated with oxidative stress, and Tha has been shown to have an antioxidant effect by affecting the levels of oxidative stress-related factors such as ROS, malondialdehyde (MDA), and superoxide dismutase (SOD).¹⁴ As a node in the center of inflammation, MYD88 serves as an adaptor between IL-1 receptor (IL-1R) or TLR family members and IL-1R-associated kinase (IRAK) through homotypic protein-protein interactions. This leads to the activation of nuclear factor kappa B (NF- κB) signaling.¹⁵ NF- κB proteins are a family of transcription factors that have significant roles in many pathological processes, including oxidative damage and inflammation.

In comparison to the NC group, the PV group exhibited higher levels of p65 protein expression and I $\kappa\text{B}\alpha$ phosphorylation (Figure 5A–C). The protein expression level of P65 and the phosphorylation level of I $\kappa\text{B}\alpha$ were decreased in the Tha treatment group compared to the PV cell model group. Compared with that in the Tha treatment group, the protein expression level of p65 was significantly elevated, and the phosphorylation level of I $\kappa\text{B}\alpha$ was significantly lowered after Tha treatment in the PV cell model group that overexpressed MyD88, an effect that was consistent with the alterations in the PV group. After the treatment of cells with 5 $\mu\text{mol/L}$ BAY11-7082 to inhibit NF- κB

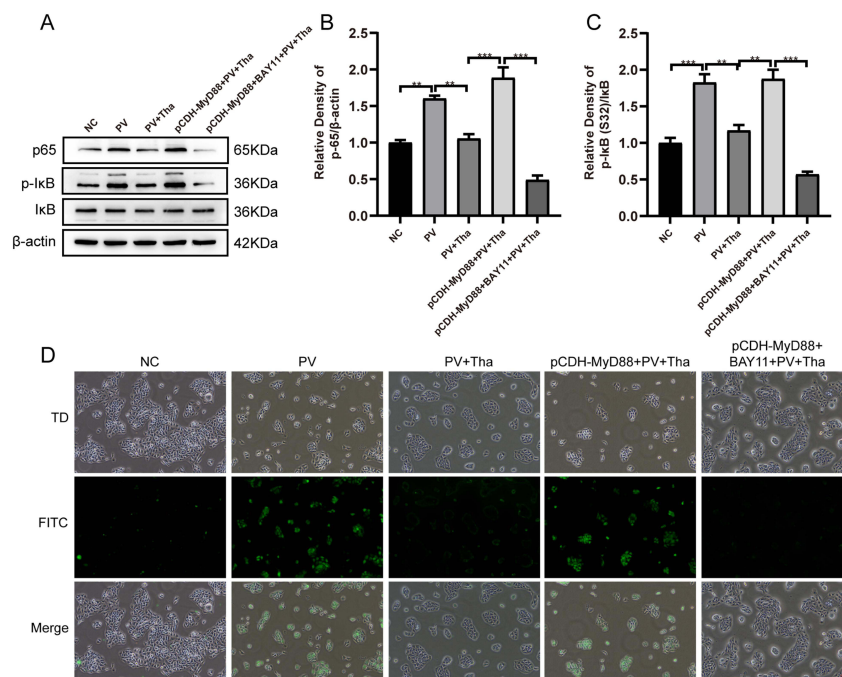


Figure 5 Continued.

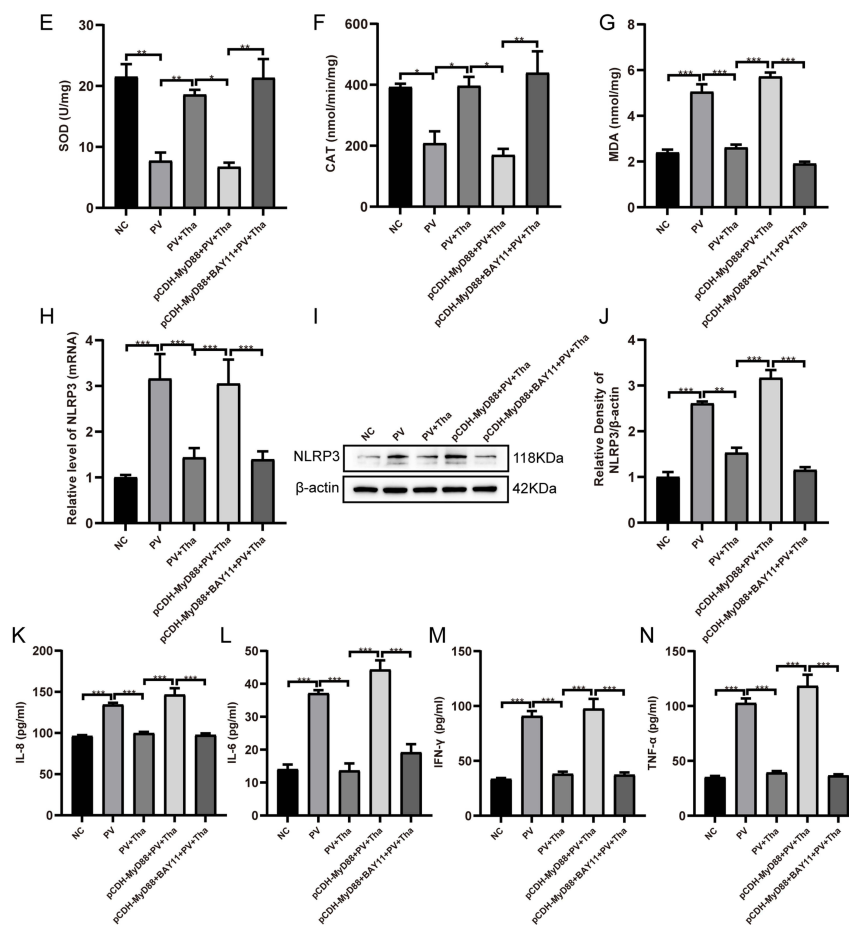


Figure 5 Overexpression of MyD88 blocked Thd effects on oxidative damage and inflammatory response by PV-IgG in HaCat cells. **(A)** HaCat cells were pretreated with NH-IgG (NC), PV-IgG (PV), PV-IgG + Thd (PV + Thd), p-CDH-MyD88-2 + PV-IgG + Thd (p-CDH-MyD88 + PV + Thd) and p-CDH-MyD88-2 + BAY11-7082 (5 μmol/L) + PV-IgG + Thd (p-CDH-MyD88 + BAY11 + PV + Thd) differently. Representative Western blots and quantification of indicated proteins in HaCat cells lysate. **(B)** PV-IgG-increased p65 expression, was reversed by Thd, overexpression of MyD88 blocked the effects of Thd on p65, using an NF-κB inhibitor BAY11-7082 (5 μmol/L) inhibited the increased p65 by overexpression MyD88 in HaCat cells. **(C)** PV-IgG-increased the level of p-IκB, was reversed by Thd, overexpression of MyD88 blocked the effects of Thd on p-IκB, using an NF-κB inhibitor BAY11-7082 (5 μmol/L) inhibited the increased p-IκB level by overexpression MyD88 in HaCat cells. **(D)** Representative ROS production in HaCat cells examined by microscopy with H2DCFDA staining. PV-IgG-increased the ROS level, was reversed by Thd, overexpression of MyD88 blocked the effects of Thd on ROS level, using an NF-κB inhibitor BAY11-7082 (5 μmol/L) inhibited the increased ROS level by overexpression MyD88 in HaCat cells. **(E)** PV-IgG-decreased the SOD level, was reversed by Thd, overexpression of MyD88 blocked the effects of Thd on SOD level, using an NF-κB inhibitor BAY11-7082 (5 μmol/L) inhibited the decreased SOD level by overexpression MyD88 in HaCat cells. **(F)** PV-IgG-decreased the CAT level, was reversed by Thd, overexpression of MyD88 blocked the effects of Thd on CAT level, using an NF-κB inhibitor BAY11-7082 (5 μmol/L) inhibited the decreased CAT level by overexpression MyD88 in HaCat cells. **(G)** PV-IgG-increased the MDA level, was reversed by Thd, overexpression of MyD88 blocked the effects of Thd on MDA level, using an NF-κB inhibitor BAY11-7082 (5 μmol/L) inhibited the increased MDA level by overexpression MyD88 in HaCat cells. **(H)** PV-IgG-increased the NLRP3 mRNA level, was reversed by Thd, overexpression of MyD88 blocked the effects of Thd on NLRP3 mRNA level, using an NF-κB inhibitor BAY11-7082 (5 μmol/L) inhibited the increased NLRP3 mRNA level by overexpression MyD88 in HaCat cells. **(I)** Representative Western blots and quantification of indicated proteins in HaCat cells lysate. **(J)** PV-IgG-increased the NLRP3 expression, was reversed by Thd, overexpression of MyD88 blocked the effects of Thd on NLRP3 expression, using an NF-κB inhibitor BAY11-7082 (5 μmol/L) inhibited the increased NLRP3 expression by overexpression MyD88 in HaCat cells. **(K–N)** PV-IgG-increased the IL-8, IL-6, IFN-γ and TNF-α levels, were reversed by Thd, overexpression of MyD88 blocked the effects of Thd on IL-8, IL-6, IFN-γ and TNF-α levels, using an NF-κB inhibitor BAY11-7082 (5 μmol/L) inhibited the increased IL-8, IL-6, IFN-γ and TNF-α levels by overexpression MyD88 in HaCat cells. Relative expression was normalized to control group. Asterisks indicate statistical significance (**p* < 0.05, ***p* < 0.01, ****p* < 0.001). Each experiment is representative of five independent experiments. The data are presented as the mean ± SEM of five separate experiments.

activation, P65 protein expression decreased, IκBα phosphorylation decreased, and the effects of MyD88 on P65 and IκBα were abolished.

Intracellular ROS can affect or be affected by the activity of NF-κB. The production of ROS was measured using the 2',7'-dichlorofluorescein-diacetate (DCFH-DA) assay, and the results showed that intracellular ROS increased in the PV model group (Figure 5D), significantly decreased in the Tha treatment group, and increased after Tha treatment in the MyD88 high expression group. After treating the cells with 5 μmol/L BAY11-7082 to inhibit NF-κB activation, followed by Tha treatment, intracellular ROS significantly decreased. SOD and other enzymes are targets of NF-κB.¹⁶ The test

results indicated that SOD and catalase (CAT) decreased in the PV model group, whereas MDA increased in this group (Figures 5E–G). After treatment, the levels recovered significantly, but no recovery was observed after Tha treatment in the high MyD88 expression group. After treating the cells with 5 $\mu\text{mol/L}$ BAY11-7082 to inhibit NF- κB activation, followed by Tha treatment, SOD and CAT recovered significantly, and MDA decreased. The I κB protein plays a crucial role in regulating NF- κB activity; I κB binds to the NF- κB protein and masks its DNA-binding domain.

TLR/MyD88 involvement may trigger the initiation of NF- κB and the activation of the NLRP3-ASC inflammasome.¹⁷ From the outcomes of PCR, it was observed that the mRNA level of NLRP3 in the PV group was elevated compared to the NC group and was recovered after Tha treatment (Figure 5H). Compared with that in the Tha treatment group, the NLRP3 mRNA level was higher in the PV cell model group in which MyD88 was overexpressed and then treated with Tha, and the NLRP3 mRNA level recovered after treatment with 5 $\mu\text{mol/L}$ BAY11-7082. The alterations observed in mRNA were in line with the Western blot results (Figures 5I and J). The level of NLRP3 was elevated in the PV group than in the NC group and recovered after Tha treatment. In contrast with the Tha treatment group, the expression of NLRP3 was higher in the PV cell model group in which MyD88 was overexpressed and then treated with Tha, and the expression of NLRP3 recovered after treatment with 5 $\mu\text{mol/L}$ BAY11-7082.

Enzyme-linked immunosorbent assays (ELISAs) were utilized to detect the levels of IFN- γ , TNF- α , IL-6, and IL-8 in the supernatant of the cell culture medium (Figures 5K–N). In comparison to those in the NC group, the concentrations of the above inflammatory factors were elevated in the PV model group and considerably lowered in the Tha treatment group. In the MYD88 high expression group, the alterations were consistent with those in the PV group after Tha treatment, and the content of the above inflammatory factors decreased after treatment with 5 $\mu\text{mol/L}$ BAY11-7082.

These findings confirm that Tha regulates the I κB /NF- κB pathway through MyD88, thereby inhibiting oxidative stress and inflammatory responses.

Tha Alleviates Acantholysis in PV-IgG-Induced Model Mice

It was further investigated whether Tha is effective in the treatment of PV. An animal model of PV was successfully constructed through the subcutaneous injection of PV-IgG. According to literature review, the construction methods of PV passive transfer mice include subcutaneous injection, intradermal injection and intraperitoneal injection of PV IgG in newborn mice.^{18,19} The concentration of PV IgG is 1.5 mg/g. Considering the thin skin of newborn mice, intradermal injection is difficult to operate and can cause artificial blisters. So we use subcutaneous injection of PV IgG (1.5 mg/g). After the subcutaneous injection of PV-IgG, compared with the mice in the phosphate-buffered saline (PBS) group and the NH-IgG group (Figure 6), mice in the PV-IgG group developed acantholysis and blisters (36 hours after PV-IgG injection). The hematoxylin-eosin (HE) staining showed acantholysis and the formation of blisters in the epidermis, with the infiltration of neutrophils and lymphocytes in the blister fluid. Direct immunofluorescence indicated intercellular reticular deposition of IgG acanthocytes. The skin of the mice in the PBS group and the NH-IgG group was normal, no acantholysis or blisters were found by HE staining, and direct immunofluorescence was negative.

After different concentrations of Tha were administered to mice, the mice in all drug administration groups survived (Figure 7). The mice in the PV group and Tha(10 mg/kg)+PV group had different degrees of skin erosion. H&E staining revealed acantholysis in mice in the PV group, and abundant neutrophil infiltration was observed in the superficial dermis. In the Tha (10 mg/kg)+PV group, acantholysis, and neutrophil infiltration were milder than those in the PV group. Direct immunofluorescence indicated IgG reticular deposition between acanthocytes in both groups of mice. The epidermis of mice in the Tha (20 mg/kg)+PV group and Tha (50 mg/kg)+PV group had no obvious erosion, and HE staining and direct immunofluorescence were normal. Immunohistochemistry was conducted for detecting the expression of MyD88 on the skin of mice in each group. It was found that the number of positive cells in the PV group was considerably higher than in the other groups (Figure 8). The Tha (10 mg/kg)+PV group also had a large number of MyD88-positive cells. The Tha (20 mg/kg)+PV group and Tha (50 mg/kg)+PV group had significantly fewer positive cells.

A large amount of neutrophil infiltration indicates an inflammatory reaction. Using immunohistochemical methods to detect NLRP3, it was found that the number of positive cells in the PV group was significantly higher than that in the other groups (Figure 8). There were also a large number of NLRP3 positive cells in the Tha (10mg/kg)+PV group, while

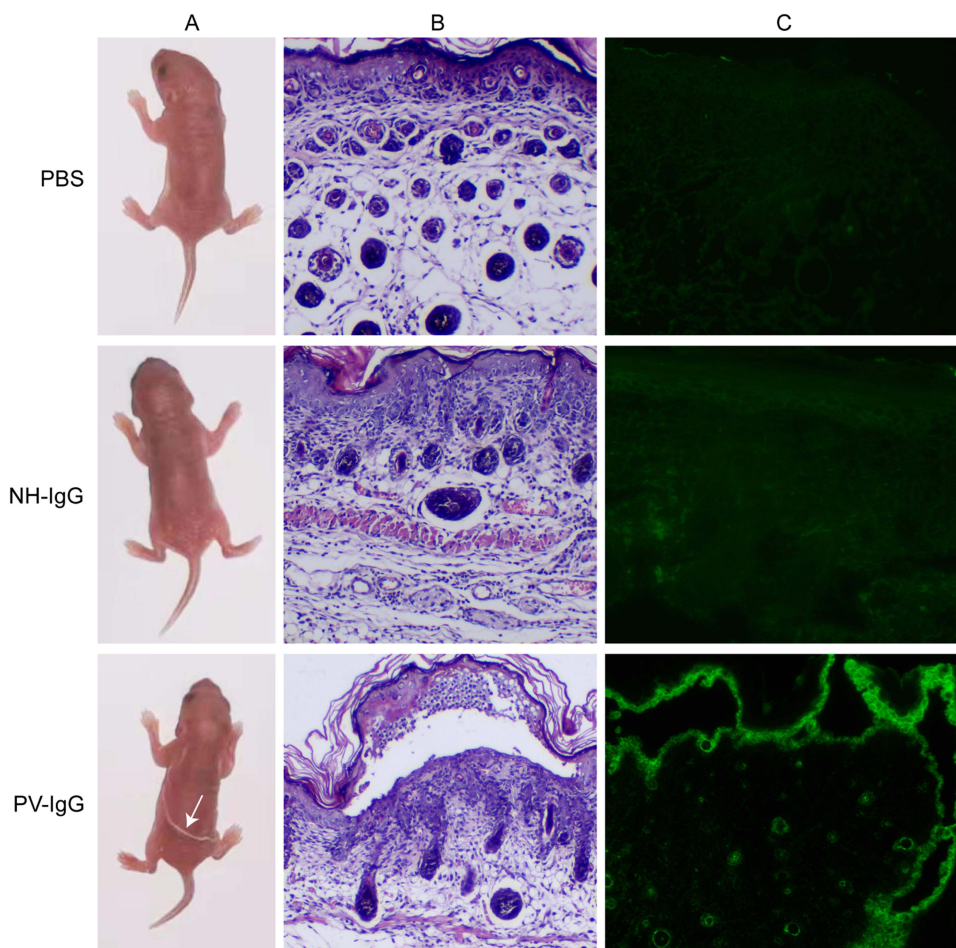


Figure 6 In vivo pathogenicity of pemphigus vulgaris (PV) IgG. Injection of neonatal mice ($n=6$ / group) with PBS, NH-IgG and PV-IgG. The PV-IgG purified from PV patients induced flaccid macroscopic blisters (**A**; lane 3; white arrows) and suprabasal splitting as seen by lesional histopathology (**B**; lane 3). No macroscopic and microscopic blistering was induced by NH-IgG (**A** and **B**; lanes 2) or PBS alone (**A** and **B**; lane 1). By direct immunofluorescence (IF) microscopy of back skin, an intercellular epidermal staining was observed in mice injected with PV-IgG (**C**; lanes 3) but not after injection of NH-IgG (**C**; lanes 2) or ETA alone (**C**, lane 1).

the positive cells in the Tha (20 mg/kg)+PV group and Tha (50 mg/kg)+PV group were significantly reduced. Terminal deoxynucleotidyl transferase dUTP nick end labeling (TUNEL) staining was conducted to evaluate the apoptosis of epidermal cells in each group of mice (**Figure 8**). The PV group had a large number of apoptotic cells. The Tha (10 mg/kg)+PV group also had a large number of apoptotic cells but fewer than that in the PV group, and there was a significant reduction in positive cells in the Tha (20 mg/kg)+PV and Tha (50 mg/kg)+PV groups.

The above results indicated that the overexpression of MyD88 was related to pemphigus and that Tha could significantly alleviate the acantholysis and inflammatory infiltration of epidermal cells in a pemphigus mouse model and inhibit the apoptosis of epidermal cells.

Discussion

PV is an immune-mediated vesicular mucocutaneous disease marked by the formation of blisters, erosions, and ulcers.²⁰ The pathological feature of pemphigus is Nikolsky's sign. In PV, autoantibodies are produced against autoantigens Dsg1 and Dsg3, disrupting the adhesion of acanthocytes to the skin and mucous membranes.²

As an immunomodulatory drug, Tha, a glutamic acid derivative, is efficacious in treating inflammatory and immune system disorders.²¹ Some patients with mild PV are treated with Tha, and its single and combined use result in good therapeutic effects and are well tolerated.⁷ Additionally, Tha also shows efficacy in treating individuals with systemic lupus erythematosus and erythema nodosum leprosum.^{22,23} The above-mentioned results suggest that Tha might become

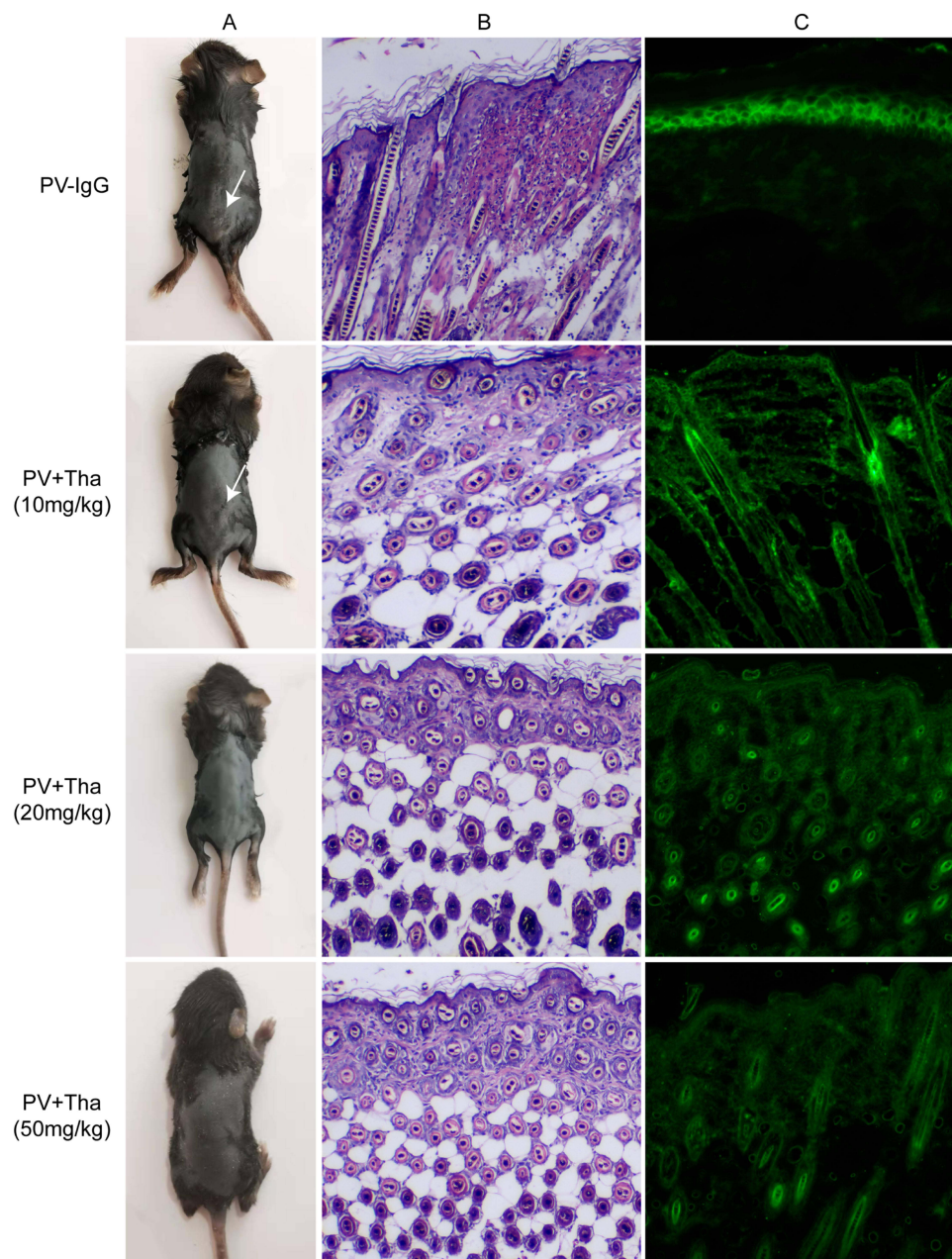


Figure 7 Effects of Thd on pathogenicity of PV-IgG. After different concentration of Tha (10 mg/kg, 20 mg/kg and 50 mg/kg) intraperitoneal injection of neonatal mice for 8 days, then injection with PV-IgG ($n=6$ /group). The PV-IgG group and Tha (10 mg/kg) treatment group induced flaccid macroscopic blisters (**A**; lane 1, 2; white arrows) and suprabasal splitting as seen by lesional histopathology (**B**; lane 1, 2). No macroscopic and microscopic blistering was induced in Tha (20 mg/kg) group and Tha (50 mg/kg) group (**A** and **B**; lanes 3, 4). By direct immunofluorescence (IF) microscopy of back skin, an intercellular epidermal staining was observed in mice injected with PV-IgG (**C**; lanes 1) but not after treatment with Tha (20 mg/kg and 50 mg/kg) (**C**; lanes 3, 4).

one of the treatment options for mild PV patients. In this experiment, Tha could restore the decrease in Dsg3 and PG caused by PV IgG, with continuous fluorescence pattern between cells being restored, further confirming that Tha has a therapeutic effect on PV.

Studies have confirmed that mitochondrial damage-mediated apoptotic events play an important role in the pathogenesis of PV, and Ca^{2+} -mediated signaling is important for PV epidermal blisters.^{24,25} Research results showed that intracellular Ca^{2+} concentration and the cell apoptosis rate increased in the PV cell model. Additionally, the expression of Bcl-2 protein decreased, whereas the expression of Caspase-3 and Bax protein increased. Thd can influence intracellular Ca^{2+} concentration.²⁶ In this study, intracellular Ca^{2+} concentration and cell apoptosis of the PV cell

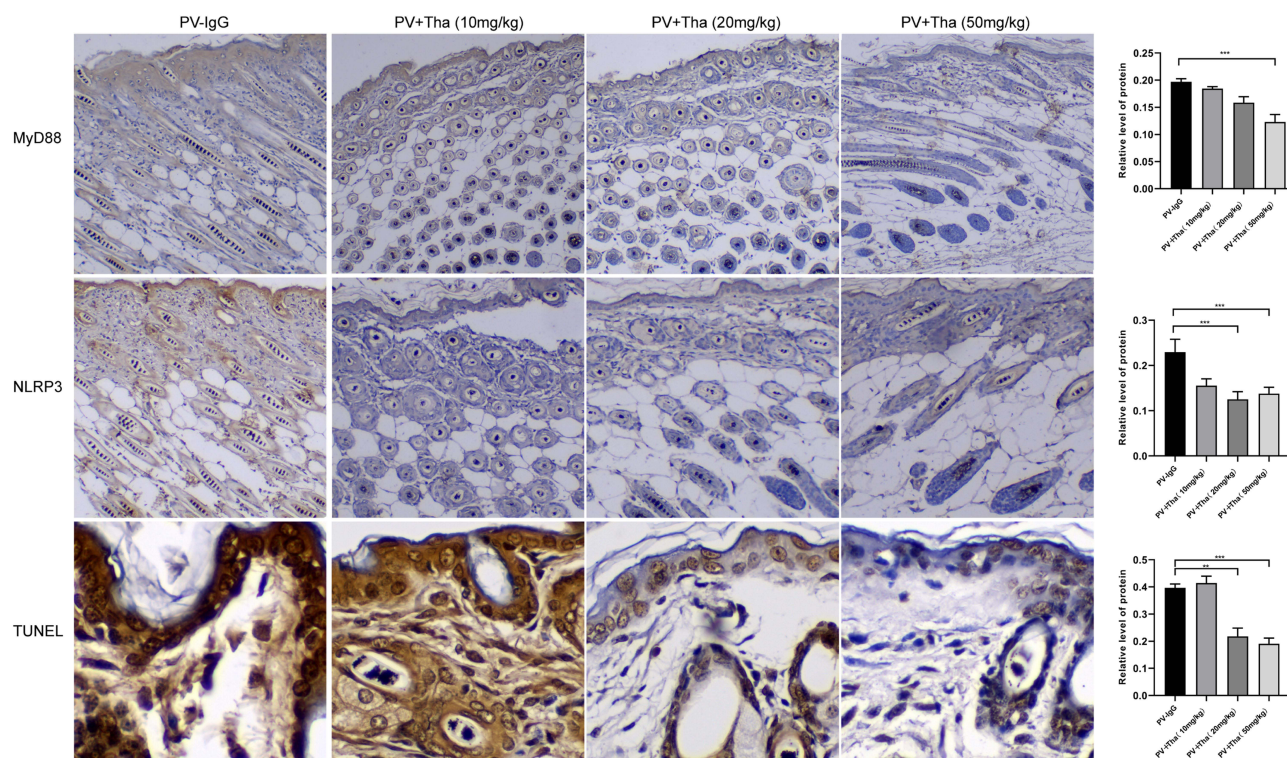


Figure 8 Effects of Thd on MyD88, NLRP3 and TUNEL staining in PV-IgG-induced PV model mice. After different concentration of Tha (10 mg/kg, 20 mg/kg and 50 mg/kg) intraperitoneal injection of neonatal mice for 8 days, then injection with PV-IgG (n=6/ group). Positivity of MyD88 staining, NLRP3 staining, TUNEL staining were detected in PV-IgG group and Thd (10 mg/kg) treatment group, whereas the Thd (20 mg/kg) group and Thd (50 mg/kg) group showed little or no staining in the skin.

model were restored by Tha. The NF- κ B signaling pathway plays an important role in PV oxidative stress injury.²⁷ As PV is an autoantibody-mediated vesicular skin disease, the level of inflammatory factors in patients is closely related to the disease.^{28,29} In this experiment, the expression of p65 protein and I κ B α phosphorylation increased in the PV cell model. Furthermore, intracellular ROS as well as IFN- γ , TNF- α , IL-6, and IL-8 levels increased in the PV cell model. Tha has been confirmed to play an antioxidant role by affecting the levels of oxidative stress-related factors such as ROS, MDA, and SOD.³⁰ As an immunosuppressant, Tha can significantly reduce the level of inflammatory factors and exert an anti-inflammatory effect.³¹ After the PV cell model was treated with Tha, the expression of P65 protein and I κ B α phosphorylation decreased, oxidative damage was alleviated, and inflammatory factors were reduced, which again verified the antioxidant and anti-inflammatory effects of Tha. Based on the above-presented results, it is speculated that Tha has a therapeutic effect on PV, which might be achieved by influencing intracellular Ca²⁺ concentration, cell apoptosis, as well as oxidative stress and inflammatory response mediated by the NF- κ B signaling pathway.

TLRs are well-characterized receptors that recognize conserved components from both own and other organisms and initiate signaling pathways of the innate immune system, thus, enhancing adaptive immune responses.³² Nearly all TLRs require MyD88 for downstream signal transduction. MyD88 functions as a central mediator of the inflammatory response and can initiate signal transduction from multiple receptors.⁹ This signaling cascade ultimately leads to the upregulation of multiple proinflammatory molecules. The TLR4/MyD88/NF- κ B pathway is involved in regulating apoptosis, oxidative stress, and inflammatory responses.³³ MyD88 influences oxidative stress by regulating the downstream NF- κ B signaling pathway.³⁴ MyD88 can regulate the concentration of intracellular Ca²⁺ by influencing the oxidation of calmodulin-dependent protein kinase II, thereby controlling apoptosis of cells.³⁵ MyD88 is a central regulatory point of inflammation, and NF- κ B initiation and NLRP3-ASC inflammasome activation can be driven by TLR/MyD88 involvement.¹⁷ Studies have reported that Tha can downregulate MyD88 level. Based on the regulatory mechanism involved in MYD88 and the pharmacological effects of Tha, this study hypothesized that the therapeutic effect of Tha on PV might be achieved through MYD88. In this experiment, MYD88 increased in the PV cell model and patient's skin tissue, and the

expression of MYD88 decreased after Tha treatment. The improvement caused by Tha after MyD88 overexpression was not obvious. Nevertheless, Tha worked by blocking calcium channels and inhibiting the NF- κ B signaling pathway in the downstream signaling pathway. Tha treatment caused an improvement in oxidative stress and inflammatory response and reduced apoptosis in the PV cell models, thus, preliminary confirming the hypothesis of the study.

As a very interesting phenomenon in this study, *in vitro* experiments found that the improvement effect in the 5 μ g/mL Tha group was the strongest, with no recovery in the 50 μ g/mL group. Moreover, we examined the effects of Tha on the viability of HaCat cells. HaCat cells were treated with different concentrations (0, 5, 10, 20, and 50 μ g/mL) of Tha. The results showed that different concentrations of Tha did not affect the cellular activity of HaCat. Therefore, we speculate that high concentrations of Tha might have inhibitory effects on certain signal transduction processes in HaCat cells. Because the purpose of this experiment was to determine the effective concentration of Tha in the treatment of PV cell models, we did not study why the 50 μ g/mL (200 μ M) group did not show recovery. However, this interesting phenomenon is worth further investigation in future experiments. Recently, a study on the effect of Tha on mast cell-mediated allergic reaction has shown that 20 μ M Tha had a significant effect.³⁶ Similarly, they did not use higher concentrations of Tha. In *in vivo* experiments, we used a PV passive transfer model in neonatal C57BL/6 mice, in which autoantibodies purified from the patients' serum bind to desmoglein of acanthocytes and induce cell-cell adhesion. Thus, by reproducing the clinical and histological characteristics of human diseases, we successfully constructed PV animal models. After Tha treatment, changes in MYD88 expression, epidermal cell apoptosis, and inflammasomes were consistent with the results of *in vitro* experiments. Unfortunately, in this part of the experiment, we failed to successfully construct MYD88 high-expressing mice and could not collect enough blood for the detection of inflammatory factors due to the small size of the newborn mice and the dependence on the mother mouse for survival. Regarding Tha treatment, we administered the drug for 8 days and then administered a subcutaneous injection of PV IgG. The main considerations are that this model exhibits dose dependency on the antibody and that the self-repairing ability is fast. This was supported by the finding that mice developed skin damage in a dose- and titer-dependent manner, and the skin damage was healed once PV IgG administration was stopped.¹

Conclusion

Through rigorous data statistical analysis and processing.³⁷ The above-discussed data suggest that Tha can reverse the decrease in Dsg3 and PG caused by PV IgG extracted from the patients' serum. The expression of MyD88 increased in the patients' skin, PV cell model, and PV mice model. Overexpression of MyD88 was associated with PV. Tha could reduce apoptosis and alleviate oxidative damage and inflammatory response induced by PV IgG in HaCaT cells through MYD88. Tha alleviated acantholysis, IgG deposition, and epidermal cell apoptosis in the mice model induced by PV IgG. We believe that this experimental result has important significance in the study of the mechanism of action of Tha in the treatment of mild PV and can provide new ideas for the development of more effective and safer treatment plans for Tha in PV treatment.

Abbreviation

Tha, Thalidomide; PV, pemphigus vulgaris; PF, pemphigus foliaceus; Dsg1, desmoglein1; Dsg3, desmoglein 3; MyD88, Myeloid differentiation primary response gene 88.

Data Sharing Statement

All the relevant data is provided within the paper and its supporting information files. The datasets analysed during the current study are available from the corresponding author on reasonable request.

Acknowledgments

Thanks to all the authors' families for their support.

Author Contributions

All authors made a significant contribution to the work reported, whether that is in the conception, study design, execution, acquisition of data, analysis and interpretation, or in all these areas; took part in drafting, revising or critically reviewing the article; gave final approval of the version to be published; have agreed on the journal to which the article has been submitted; and agree to be accountable for all aspects of the work.

Disclosure

The authors declare that the research was conducted in the absence of any commercial or financial relationships that could be construed as a potential conflict of interest.

References

1. Anhalt GJ, Labib RS, Voorhees JJ, Beals TF, Diaz LA. Induction of pemphigus in neonatal mice by passive transfer of IgG from patients with the disease. *N Engl J Med*. 1982;306(20):1189–1196. doi:10.1056/NEJM198205203062001
2. Das D, Akhtar S, Kurra S, Gupta S, Sharma A. Emerging role of immune cell network in autoimmune skin disorders: an update on pemphigus, vitiligo and psoriasis. *Cytokine Growth Factor Rev*. 2019;45(35–44). doi:10.1016/j.cytogfr.2019.01.001
3. Egami S, Yamagami J, Amagai M. Autoimmune bullous skin diseases, pemphigus and pemphigoid. *J Allergy Clin Immunol*. 2020;145(4):1031–1047. doi:10.1016/j.jaci.2020.02.013
4. Santoro FA, Stoopler ET, Werth VP. Pemphigus. *Dent Clin North Am*. 2013;57(4):597–610. doi:10.1016/j.cden.2013.06.002
5. Tavakolpour S, Alesaeidi S, Darvishi M, et al. A comprehensive review of rituximab therapy in rheumatoid arthritis patients. *Clin Rheumatol*. 2019;38(11):2977–2994. doi:10.1007/s10067-019-04699-8
6. Domingo S, Sole C, Moline T, Ferrer B, Cortes-Hernandez J. Thalidomide exerts anti-inflammatory effects in cutaneous lupus by Inhibiting the IRF4/NF- κ B and AMPK1/mTOR pathways. *Biomedicines*. 2021;9(12):1857. doi:10.3390/biomedicines9121857
7. Wang J, Zhang Y, Pan M. Thalidomide as a potential adjuvant treatment for paraneoplastic pemphigus: a single-center experience. *Dermatol Ther*. 2020;33(6):e14353. doi:10.1111/dth.14353
8. Zhang B, Mao X, Zhao W, Jin H, Li L. Successful treatment with thalidomide for pemphigus vulgaris. *Ther Adv Chronic Dis*. 2020;11(2040622320916023):2040622320916023. doi:10.1177/2040622320916023
9. Deguine J, Barton GM. MyD88: a central player in innate immune signaling. *F1000Prime Rep*. 2014;6(97). doi:10.12703/P6-97
10. Noman AS, Koide N, Hassan F, et al. Thalidomide inhibits lipopolysaccharide-induced tumor necrosis factor- α production via down-regulation of MyD88 expression. *Innate Immun*. 2009;15(1):33–41. doi:10.1177/1753425908099317
11. Schmitt T, Pircher J, Steinert L, et al. Dsg1 and Dsg3 composition of desmosomes across human epidermis and alterations in pemphigus vulgaris patient skin. *Front Immunol*. 2022;13(884241). doi:10.3389/fimmu.2022.884241
12. Sharma BR, Karki R, Lee E, Zhu Q, Gurung P, Kanneganti TD. Innate immune adaptor MyD88 deficiency prevents skin inflammation in SHARPIN-deficient mice. *Cell Death Differ*. 2019;26(4):741–750. doi:10.1038/s41418-018-0159-7
13. Singh MV, Swaminathan PD, Luczak ED, Kutschke W, Weiss RM, Anderson ME. MyD88 mediated inflammatory signaling leads to CaMKII oxidation, cardiac hypertrophy and death after myocardial infarction. *J Mol Cell Cardiol*. 2012;52(5):1135–1144. doi:10.1016/j.yjmcc.2012.01.021
14. Dong X, Li X, Li M, Chen M, Fan Q, Wei W. Antiinflammation and antioxidant effects of thalidomide on pulmonary fibrosis in mice and human lung fibroblasts. *Inflammation*. 2017;40(6):1836–1846. doi:10.1007/s10753-017-0625-2
15. Nakano H, Nakajima A, Sakon-Komazawa S, Piao JH, Xue X, Okumura K. Reactive oxygen species mediate crosstalk between NF- κ B and JNK. *Cell Death Differ*. 2006;13(5):730–737. doi:10.1038/sj.cdd.4401830
16. Morgan MJ, Liu ZG. Crosstalk of reactive oxygen species and NF- κ B signaling. *Cell Res*. 2011;21(1):103–115. doi:10.1038/cr.2010.178
17. Jiang S, Maphis NM, Binder J, et al. Proteopathic tau primes and activates interleukin-1 β via myeloid-cell-specific MyD88- and NLRP3-ASC-inflammasome pathway. *Cell Rep*. 2021;36(12):109720. doi:10.1016/j.celrep.2021.109720
18. Berkowitz P, Hu P, Warren S, Liu Z, Diaz LA, Rubenstein DS. p38MAPK inhibition prevents disease in pemphigus vulgaris mice. *Proc Natl Acad Sci U S A*. 2006;103(34):12855–12860. doi:10.1073/pnas.0602973103
19. Schulze K, Galichet A, Sayar BS, et al. An adult passive transfer mouse model to study desmoglein 3 signaling in pemphigus vulgaris. *J Invest Dermatol*. 2012;132(2):346–355. doi:10.1038/jid.2011.299
20. Buonavoglia A, Leone P, Dammacco R, et al. Pemphigus and mucous membrane pemphigoid: an update from diagnosis to therapy. *Autoimmun Rev*. 2019;18(4):349–358. doi:10.1016/j.autrev.2019.02.005
21. Wirsching HG, Weller M, Balabanov S, Roth P. Targeted therapies and immune checkpoint inhibitors in primary CNS lymphoma. *Cancers*. 2021;13(12):3073. doi:10.3390/cancers13123073
22. Yuki EFN, Silva CA, Aikawa NE, et al. Thalidomide and lenalidomide for refractory systemic/cutaneous lupus erythematosus treatment: a narrative review of literature for clinical practice. *J Clin Rheumatol*. 2021;27(6):248–259. doi:10.1097/RHU.0000000000001160
23. Lu Q, Long H, Chow S, et al. Guideline for the diagnosis, treatment and long-term management of cutaneous lupus erythematosus. *J Autoimmun*. 2021;123(102707):102707. doi:10.1016/j.jaut.2021.102707
24. Wei B, Li F. Mechanisms of Trx2/ASK1-mediated mitochondrial injury in pemphigus vulgaris. *Biomed Res Int*. 2021;2021(2471518):1–10. doi:10.1155/2021/2471518
25. Schmitt T, Egu DT, Walter E, et al. Ca(2+) signalling is critical for autoantibody-induced blistering of human epidermis in pemphigus. *Br J Dermatol*. 2021;185(3):595–604. doi:10.1111/bjd.20091
26. Enomoto N, Takei Y, Hirose M, et al. Thalidomide prevents alcoholic liver injury in rats through suppression of Kupffer cell sensitization and TNF- α production. *Gastroenterology*. 2002;123(1):291–300. doi:10.1053/gast.2002.34161
27. Liang J, Zeng X, Halifu Y, et al. Blocking RhoA/ROCK inhibits the pathogenesis of pemphigus vulgaris by suppressing oxidative stress and apoptosis through TAK1/NOD2-mediated NF- κ B pathway. *Mol Cell Biochem*. 2017;436(1–2):151–158. doi:10.1007/s11010-017-3086-x

28. Mortazavi H, Babaeijandaghi F, Akbarzadeh M, et al. The influence of systemic therapy on the serum levels of IL-6 and IL-8 in pemphigus vulgaris. *J Eur Acad Dermatol Venereol*. 2013;27(3):387–390. doi:10.1111/j.1468-3083.2011.04319.x
29. Kowalski EH, Kneibner D, Kridin K, Amber KT. Serum and blister fluid levels of cytokines and chemokines in pemphigus and bullous pemphigoid. *Autoimmun Rev*. 2019;18(5):526–534. doi:10.1016/j.autrev.2019.03.009
30. De Logu F, Trevisan G, Marone IM, et al. Oxidative stress mediates thalidomide-induced pain by targeting peripheral TRPA1 and central TRPV4. *BMC Biol*. 2020;18(1):197. doi:10.1186/s12915-020-00935-9
31. Talaat R, El-Sayed W, Agwa HS, Gamal-Eldeen AM, Moawia S, Zahran MA. Anti-inflammatory effect of thalidomide dithiocarbamate and dithioate analogs. *Chem Biol Interact*. 2015;238:74–81. doi:10.1016/j.cbi.2015.05.017
32. He WT, Zhang LM, Li C, et al. Short-term MyD88 inhibition ameliorates cardiac graft rejection and promotes donor-specific hyporesponsiveness of skin grafts in mice. *Transpl Int*. 2016;29(8):941–952. doi:10.1111/tri.12789
33. Zhang Q, Wang L, Wang S, et al. Signaling pathways and targeted therapy for myocardial infarction. *Signal Transduct Target Ther*. 2022;7(1):78. doi:10.1038/s41392-022-00925-z
34. Luo S, Gong J, Cao X, Liu S. Ligustilide modulates oxidative stress, apoptosis, and immunity to avoid pathological damages in bleomycin induced pulmonary fibrosis rats via inactivating TLR4/MyD88/NF-KB P65. *Ann Transl Med*. 2020;8(15):931. doi:10.21037/atm-20-4233
35. Faridvand Y, Nozari S, Vahedian V, et al. Nrf2 activation and down-regulation of HMGB1 and MyD88 expression by amnion membrane extracts in response to the hypoxia-induced injury in cardiac H9c2 cells. *Bio Pharmaco*. 2019;109(360–368):360–368. doi:10.1016/j.biopha.2018.10.035
36. Chang HW, Sim KH, Lee YJ. Thalidomide attenuates mast cell activation by upregulating SHP-1 signaling and interfering with the action of CRBN. *Cells*. 2023;12(3):469. doi:10.3390/cells12030469
37. Panos GD, Boeckler FM. Statistical analysis in clinical and experimental medical research: simplified guidance for authors and reviewers. *Drug Des Devel Ther*. 2023;17(1959–1961):1959–1961. doi:10.2147/DDDT.S427470

Drug Design, Development and Therapy

Dovepress

Publish your work in this journal

Drug Design, Development and Therapy is an international, peer-reviewed open-access journal that spans the spectrum of drug design and development through to clinical applications. Clinical outcomes, patient safety, and programs for the development and effective, safe, and sustained use of medicines are a feature of the journal, which has also been accepted for indexing on PubMed Central. The manuscript management system is completely online and includes a very quick and fair peer-review system, which is all easy to use. Visit <http://www.dovepress.com/testimonials.php> to read real quotes from published authors.

Submit your manuscript here: <https://www.dovepress.com/drug-design-development-and-therapy-journal>